Medical Physics
The International Journal of Medical Physics Research and Practice

From physical dose constraints to equivalent uniform dose constraints in inverse radiotherapy planning

Christian Thieke, Thomas Bortfeld, Andrzej Niemierko, and Simeon Nill

Citation: Medical Physics **30**, 2332 (2003); doi: 10.1118/1.1598852
View online: http://dx.doi.org/10.1118/1.1598852
View Table of Contents: http://scitation.aip.org/content/aapm/journal/medphys/30/9?ver=pdfcov
Published by the American Association of Physicists in Medicine

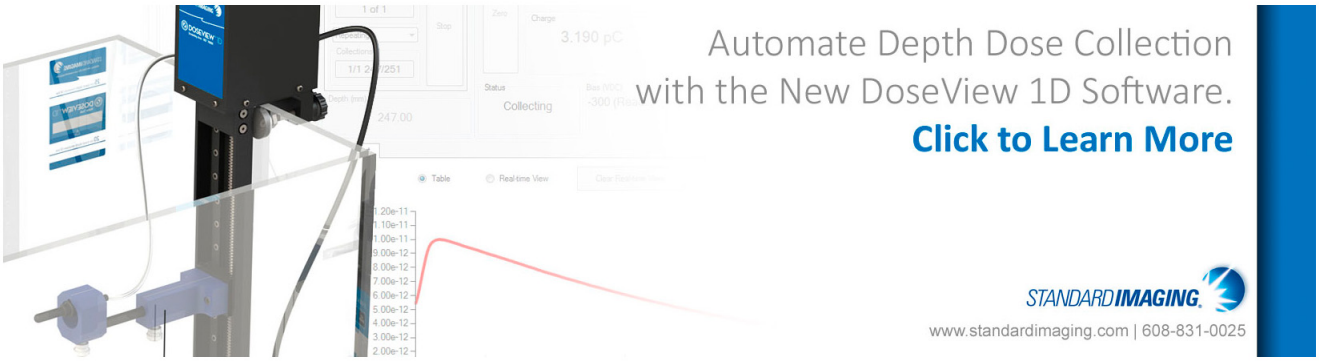

From physical dose constraints to equivalent uniform dose constraints in inverse radiotherapy planning

Christian Thieke
Department of Radiation Oncology, Massachusetts General Hospital and Harvard Medical School, Boston, Massachusetts and Department of Medical Physics, Deutsches Krebsforschungszentrum, Heidelberg, Germany

Thomas Bortfeld and Andrzej Niemierko
Department of Radiation Oncology, Massachusetts General Hospital and Harvard Medical School, Boston, Massachusetts

Simeon Nill
Department of Medical Physics, Deutsches Krebsforschungszentrum, Heidelberg, Germany

(Received 19 November 2002; revised 17 June 2003; accepted for publication 19 June 2003; published 21 August 2003)

Optimization algorithms in inverse radiotherapy planning need information about the desired dose distribution. Usually the planner defines physical dose constraints for each structure of the treatment plan, either in form of minimum and maximum doses or as dose-volume constraints. The concept of equivalent uniform dose (EUD) was designed to describe dose distributions with a higher clinical relevance. In this paper, we present a method to consider the EUD as an optimization constraint by using the method of projections onto convex sets (POCS). In each iteration of the optimization loop, for the actual dose distribution of an organ that violates an EUD constraint a new dose distribution is calculated that satisfies the EUD constraint, leading to voxel-based physical dose constraints. The new dose distribution is found by projecting the current one onto the convex set of all dose distributions fulfilling the EUD constraint. The algorithm is easy to integrate into existing inverse planning systems, and it allows the planner to choose between physical and EUD constraints separately for each structure. A clinical case of a head and neck tumor is optimized using three different sets of constraints: physical constraints for all structures, physical constraints for the target and EUD constraints for the organs at risk, and EUD constraints for all structures. The results show that the POCS method converges stable and given EUD constraints are reached closely. [DOI: 10.1118/1.1598852]

Key words: equivalent uniform dose, inverse planning, optimization constraints, projection onto convex sets

I. INTRODUCTION

In inverse treatment planning for intensity-modulated radiotherapy, the planner defines certain constraints for the desired dose distribution, and in an optimization process the computer tries to find the treatment setup that matches the constraints as closely as possible. In most inverse planning programs, the planner predefines the number and directions of the treatment beams, and only the beam's intensity profiles are optimized. Some experimental systems also include the number and directions of beams into the optimization (e.g., Ref. 1). Common constraints for the optimization are minimum and maximum doses for target structures and maximum doses for normal structures, each in conjunction with a penalty factor.[2] The penalty factors, also called weight factors, determine the impact of a constraint violation onto the optimization. The target volume and essential organs at risk like the spinal cord usually have high penalty factors, whereas less important structures might be considered with a lower priority.

These physical dose constraints allow the implementation of fast converging and robust gradient optimization algorithms. However, finding the best parameter setting is nonintuitive. Because often the dose constraints cannot be fulfilled for every single voxel, the penalty factors have a great impact on the optimization result. In these cases, the prescribed maximum dose loses its original meaning of a real constraint and is used as a mere steering parameter for the optimization outcome. Balancing the maximum/minimum constraints and their penalties is a trial and error process with several optimization runs.

For some organs at risk, a maximum dose constraint is not meaningful at all. Parallel organs like liver, lung and kidneys show a distinct volume effect, i.e., the tolerance dose depends on the irradiated volume fraction. If only a small fraction of those organs is irradiated, the tolerance dose is considerably higher than for larger irradiated fractions. To consider volume effects in a physical dose-constrained optimization, the planner can define dose volume histogram (DVH) constraints, i.e., instead of a maximum dose, the constraints are formulated in the form ''not more than x% of the organ are allowed to receive more than y Gy,'' see e.g., Ref. 3. Usually several DVH constraints have to be defined for one organ. This increases the number of parameters to be defined by the treatment planner, and it may exclude solu-

tions that keep organs at risk inside the tolerance, but that have a different shape of the DVH.

To overcome the difficulties of physical dose constrained optimization, the equivalent uniform dose (EUD) is a promising concept. The EUD is the homogeneous dose inside an organ that has the same clinical effect as a given, arbitrary dose distribution. Depending on the clinical endpoint, there can be different EUD values for the same dose inside an organ, e.g., for pneumonitis and fibrosis in the lung. The EUD model used in this work is the generalized mean of the dose values, as proposed in Refs. 4 and 5. It applies both to target structures and organs at risk. The model parameters applied here were derived from commonly used estimations of organ tolerance doses.[6] For targets, the EUD is mostly determined by the lowest dose values. In organs at risk that are organized in parallel, the EUD is near the mean dose, whereas in serial organs at risk the EUD is more dominated by the maximum dose values.

The concept of EUD is useful for inverse planning because it reduces any complex, three-dimensional dose distribution to one single number that can be handled by an optimization algorithm. When used as an optimization constraint, there is only one value to be defined by the treatment planner. Volume effects and other biological effects are taken into account. The EUD is still in the dose domain, and therefore a familiar evaluation parameter for treatment planners. Because it is a scalar, EUD also facilitates the ranking of different inhomogeneous dose distributions.

In Ref. 7, the EUD was used for inverse treatment planning as a parameter in a sigmoid dose-effect curve that resembles the basic shape of TCP/NTCP models.

In this work, we implemented the EUD directly as an optimization constraint without assuming any dose-effect relationships. In the following, we describe the mathematical aspects of the implementation, show the differences between physical dose constrained and EUD constrained optimization, and discuss the clinical application.

II. MATERIAL AND METHODS

The calculation platform for our investigation is a new inverse planning system developed at the German Cancer Research Center[8] based on KonRad.[9] As an initial step outside of the optimization loop, the dose contribution of every beam element (bixel) j to every voxel i is stored for unit fluence in a matrix D_{ij}. When the beam weights $\mathbf{w}=(w_1,\ldots,w_M)$ are changed during the iterative optimization, the dose $\mathbf{d}_T=(d_1,\ldots,d_{N_T})$ can then be calculated through

$$d_i=\sum_{j=1}^{M} D_{ij}w_j, \quad i=1,...,N_T. \tag{1}$$

M is the number of bixels, and N_T the total number of voxels. Because the matrix D has to be calculated only once, accurate dose engines like superposition algorithms can be integrated into the inverse planning process.[10] Several techniques exist to reduce the matrix size and therefore memory requirements and computation time without sacrificing accuracy.[11,12]

The planning system uses a quasi-Newton gradient technique to optimize the fluence maps. The objective function is defined as

$$F=\sum_{i=1}^{N_T} s_i(d_i-d_i^{\text{pres}})^2. \tag{2}$$

d_i^{pres} and s_i are the desired dose for the voxel i and the associated penalty factor, based on the planner's prescription and the current dose. For minimum and maximum dose constraints, d_i^{pres} and s_i are given by

$$(d_i^{\text{pres}},s_i)=\begin{cases}(d_i^{\min},s_i^{\min}) & \text{if } d_i<d_i^{\min},\\ (d_i,0) & \text{if } d_i^{\min}\leqslant d_i\leqslant d_i^{\max},\\ (d_i^{\max},s_i^{\max}) & \text{if } d_i>d_i^{\max}.\end{cases} \tag{3}$$

$(d_i^{\min},s_i^{\min})$ and $(d_i^{\max},s_i^{\max})$ are the minimum and maximum physical dose constraints and penalty factors for voxel i. Note that the system internally works with individual settings for each voxel. The planner usually defines the dose constraints and penalties only separately for each structure (targets/organs at risk), which are then assigned to all voxels belonging to the particular structure. Naturally, for organs at risk there is no minimum dose constraint.

DVH constraints are considered by an extension of the above concept, whereby up to 5 DVH constraint points per structure are transformed into adequately chosen values of d_i^{pres}.[3]

The iterative update of the beam weights from iteration (t) to iteration $(t+1)$ is given by

$$w_j^{(t+1)}=\left[w_j^{(t)}-\alpha\left(\frac{\mathrm{d}F}{\mathrm{d}w_j}\Big/\frac{\mathrm{d}^2F}{\mathrm{d}w_j^2}\right)\right]_+ =\left[w_j^{(t)}-\alpha\frac{\Sigma_{i=1}^{N}2s_i(d_i-d_i^{\text{pres}})D_{ij}}{\Sigma_{i=1}^{N}2s_iD_{ij}^2}\right]_+. \tag{4}$$

α is a damping factor to ensure convergence, and because the fluence has to be non-negative, the operator

$$[x]_+=\begin{cases}x & \text{if } x\geqslant 0,\\ 0 & \text{if } x<0\end{cases} \tag{5}$$

is used.

The handling of physical dose constraints is also illustrated in Fig. 1. It shows the DVH of a dose distribution in an organ at risk at some arbitrary step of the iterative optimization. One DVH constraint and a maximum physical dose constraint are defined for this organ, and both are violated by the actual dose distribution. The planning system then generates the arrays $\mathbf{d}^{\text{pres}}$ and $\mathbf{s}$ in a way that only those voxels violating the constraints contribute to the objective function. For all other voxels the new prescribed dose equals the actual dose. The actual dose distribution is modified as little as possible, but also as much as necessary to match all constraints. This concept has proven to result in a fast and stable optimization. It was our motivation to implement EUD con-

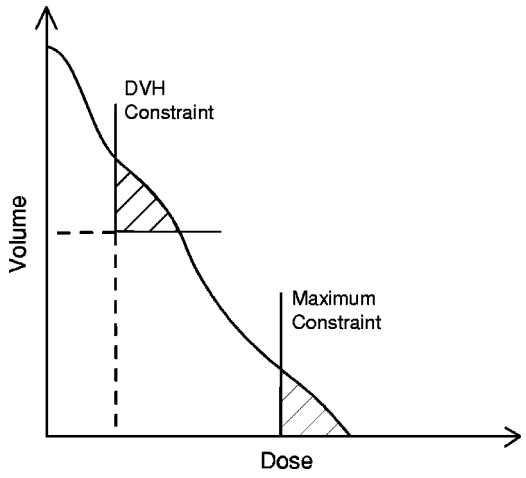

FIG. 1. Consideration of maximum dose and DVH constraints in inverse planning.

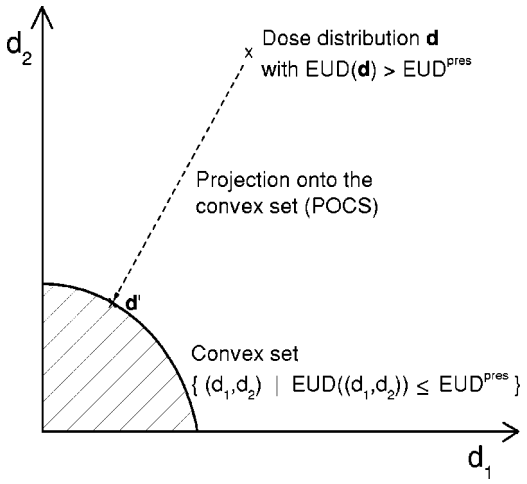

FIG. 2. The principle of projection onto convex sets (POCS).

straints into the system in a way that is compatible with the existing concept and that keeps most parts of the established algorithm unchanged.

The EUD model we use is given by (see Ref. 4)

$$\mathrm{EUD}(\mathbf{d})=\left(\frac{1}{N}\sum_{i=1}^{N} d_i^a\right)^{1/a}. \tag{6}$$

Originally, the concept of EUD dealt with the effect of radiation in tumor volumes only.[5] Equation (6), sometimes also referred to as ''generalized EUD (gEUD),'' extends this concept and can be applied both to tumor target volumes and organs at risk.[4] Whereby it keeps its original meaning of statistical cell-killing effects (not considering fractionation) for tumors, for organs at risk it is merely an empirical model that has to be fitted to clinically reported tolerance doses. The method of fitting the model to clinical data and a comparison to an alternative EUD model is reported in Ref. 13. The EUD is calculated separately for each structure. Therefore, in the following the dose vector $\mathbf{d}$ is restricted to those voxels belonging to the particular structure and has N elements, $\mathbf{d}=(d_1,\ldots,d_N)$. a is the tissue-specific parameter, which is negative for target structures and positive for organs at risk. For $a=1$, the EUD equals the mean dose, and for $a=\infty$ the EUD equals the maximum of the dose values d_i. More information about this EUD model and its mathematical properties can be found in Ref. 7.

Let us now assume that at any stage during the optimization we have a dose distribution $\mathbf{d}$ inside the organ that violates a predefined EUD constraint, e.g., $\mathrm{EUD}(\mathbf{d})>\mathrm{EUD}^{\max}$ for an organ at risk. In analogy to the handling of physical dose constraints described above, we now want to find a new dose distribution $\mathbf{d}'$ that fulfils the constraint, i.e., $\mathrm{EUD}(\mathbf{d}')\leqslant\mathrm{EUD}^{\max}$, and at the same time is as close to $\mathbf{d}$ as possible. The elements of $\mathbf{d}'$, $(d_1',\ldots,d_N')$, can then be used as physical dose constraints in the array $\mathbf{d}^{\mathrm{pres}}$, see Eq. (2).

To find $\mathbf{d}'$, we make use of a mathematical property of the EUD formula, namely its convexity for $a<0$ and $a\geqslant 1$.[14] Convexity means that for two given dose distributions within the constraint, any convex combination of these two also satisfies the constraint

$$\alpha\,\mathrm{EUD}(\mathbf{d}_1)+(1-\alpha)\mathrm{EUD}(\mathbf{d}_2)\leqslant\mathrm{EUD}^{\max}, \tag{7}$$

$$\text{for } \mathrm{EUD}(\mathbf{d}_1),\ \mathrm{EUD}(\mathbf{d}_2)\leqslant\mathrm{EUD}^{\max},\ 0\leqslant\alpha\leqslant 1,\ a\geqslant 1, \tag{8}$$

and

$$\alpha\,\mathrm{EUD}(\mathbf{d}_1)+(1-\alpha)\mathrm{EUD}(\mathbf{d}_2)\geqslant\mathrm{EUD}^{\min}, \tag{9}$$

$$\text{for } \mathrm{EUD}(\mathbf{d}_1),\ \mathrm{EUD}(\mathbf{d}_2)\geqslant\mathrm{EUD}^{\min},\ 0\leqslant\alpha\leqslant 1,\ a<0. \tag{10}$$

In other words, all dose distributions that satisfy a given EUD constraint form a convex set inside the N-dimensional dose space. This property is essential to make the projection from $\mathbf{d}$ to $\mathbf{d}'$ unique. It is called a projection onto a convex set (POCS),[15,16] a technique known from other applications, e.g., in image restoration.[17] POCS has also already been used in radiotherapy planning,[18] especially as an alternative method for considering DVH constraints.[19] Figure 2 illustrates the principle. For reasons of clarity, an organ with only two voxels ($N=2$) is shown, so that every dose distribution $\mathbf{d}=(d_1,d_2)$ can be represented by a point on the plane. We look at an organ at risk with an EUD parameter of $a=2$ and a prescribed maximum constraint $\mathrm{EUD}^{\mathrm{pres}}$. All dose distributions fulfilling the constraint form a convex set that includes $\mathbf{d}=(0,0)$ and has a border forming a circle segment from $\mathbf{d}=(\sqrt{2}\cdot\mathrm{EUD}^{\mathrm{pres}},0)$ to $\mathbf{d}=(0,\sqrt{2}\cdot\mathrm{EUD}^{\mathrm{pres}})$. For other organ parameters a, the border would have a different shape, but would be still convex. Also shown in Fig. 2 is a dose distribution $\mathbf{d}$ that violates the constraint and its projection to the nearest point of the convex set, $\mathbf{d}'$. It is clear that $\mathbf{d}'$ will fulfill the EUD constraint exactly and does not go beyond that, i.e., we will have $\mathrm{EUD}(\mathbf{d}')=\mathrm{EUD}^{\mathrm{pres}}$ instead of the inequality used so far. The same applies for minimum EUD constraints, so the following calculation is valid for both maximum and minimum constraints.

To calculate $\mathbf{d}'$, we have to find the minimum of

$$f(\mathbf{d}')=\sum_{i=1}^{N}(d_i-d_i')^2 \tag{11}$$

under the constraint $\mathrm{EUD}(\mathbf{d}')=\mathrm{EUD}^{\mathrm{pres}}$. This is a classical setup for the use of Lagrange multipliers. We define a Lagrange function

$$L(\mathbf{d}')=f(\mathbf{d}')+\lambda(\mathrm{EUD}^{\mathrm{pres}}-\mathrm{EUD}(\mathbf{d}')) \tag{12}$$

and set the gradient to zero,

$$\left(\frac{\partial L}{\partial \mathbf{d}'}\right)_j=-2(d_j-d_j')-\frac{1}{N}\lambda d_j'^{a-1}\left(\frac{1}{N}\sum_{i=1}^{N}d_i'^{a}\right)^{(1/a)-1}=0 \tag{13}$$

$$\Rightarrow \frac{d_j-d_j'}{d_j'^{a-1}}=-\frac{\lambda}{2N}\left(\frac{1}{N}\sum_{i=1}^{N}d_i'^{a}\right)^{(1/a)-1},\quad j=1,..,N. \tag{14}$$

The explicit value of the Lagrange multiplier λ is unknown, but it can be seen from Eq. (14) that for every voxel index j we have a constant expression for d_j',

$$\frac{d_j-d_j'}{d_j'^{a-1}}=\mathrm{const},\quad j=1,...,N. \tag{15}$$

The value of const that is exact for $a=1$ and $a=2$ and approximately correct for all other values of a is given by

$$\frac{d_j-d_j'}{d_j'^{a-1}}\approx\frac{\mathrm{EUD}(\mathbf{d})-\mathrm{EUD}^{\mathrm{pres}}}{(\mathrm{EUD}^{\mathrm{pres}})^{(a-1)}}. \tag{16}$$

Equation (16) is an implicit definition for $\mathbf{d}'$. In practice, this is as good as an explicit definition, because each element d_j' can be calculated in a short and fast iterative subroutine. It is interesting to note that for $a=1$ the dose is just shifted by $\mathrm{const}=(\mathrm{EUD}(\mathbf{d})-\mathrm{EUD}^{\mathrm{pres}})$, and for $a=2$ the relative change of the dose is constant.

When projecting to a lower EUD, for every j we have

$$d_j'\leq d_j,\quad j=1,...,N, \tag{17}$$

and when projecting to a higher EUD, used for target structures in case the minimal EUD constraint is violated, we have

$$d_j'\geq d_j,\quad j=1,...,N. \tag{18}$$

If only a minimum EUD constraint is used for target structures, Eq. (18) would lead to very high doses in some target voxels because they would never be actively reduced. To assure target dose homogeneity, we therefore consider the target also as an organ at risk and prescribe a maximum EUD. There has to be a separate target parameter $a\geq 1$ for the maximum EUD constraint to ensure the convexity. The use of both minimum and maximum EUD constraints for target structures implies that there might be two projections directly after one another to obtain $\mathbf{d}'$: First, to a higher EUD in case the minimum EUD constraint is violated, and starting from this dose distribution a projection down to the maximum constraint.

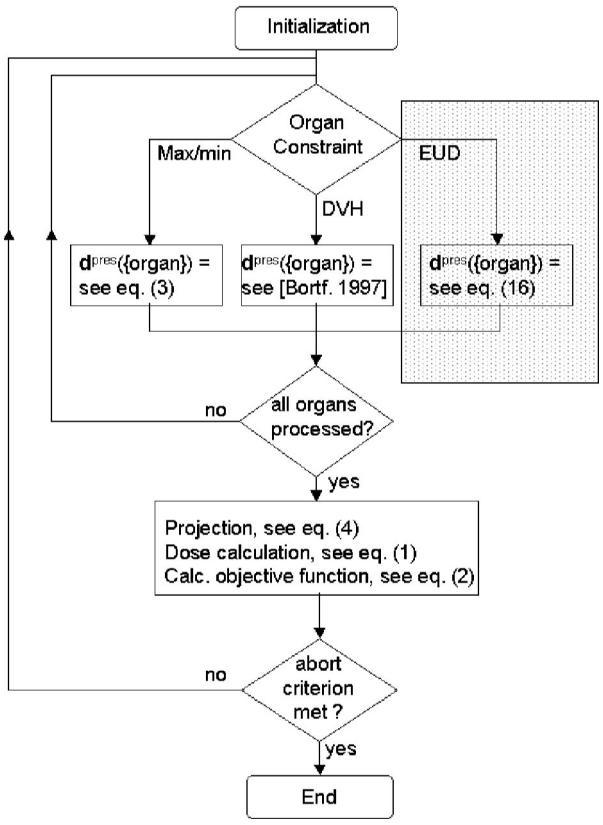

FIG. 3. Optimization loop of the inverse planning program. To add the option of EUD-constrained optimization, simply a new branch has to be added to the generation of $\mathbf{d}^{\mathrm{pres}}$ (marked by the dotted background).

In summary, the EUD constraint defined by the planner is internally transformed into physical dose constraints for each individual voxel. In practice Eq. (3) is replaced by Eq. (16) for the particular organ. This is illustrated in the flowchart in Fig. 3. In each iteration, a dose distribution $\mathbf{d}^{\mathrm{pres}}$ is generated, based on the current dose and individual for each voxel. $\mathbf{d}^{\mathrm{pres}}$ is generated by processing organ after organ, and so it is possible to chose different constraint types (either physical max/min, DVH or EUD) separately for each of them. The ability of considering EUD constraints can be implemented by simply adding a branch to the generation of $\mathbf{d}^{\mathrm{pres}}$ (marked by the dotted background in Fig. 3). It should be emphasized that the POCS projection is done in the dose domain. In standard POCS algorithms the projections are carried out sequentially (which would mean optimizing organ after organ), but in our case there are simultaneous projections for all organs. Since the critical organs do not overlap, the projections are completely independent, and there is no difference between these two approaches. For target structures with maximum and minimum EUD constraints however, there is a difference, which will be referred to in the discussion section. The POCS projection is followed by the scaled gradient projection [Eq. (4)] between the dose and the intensities. The objective function and all other parts of the optimization algorithm are retained without change. The abort criterion is met if the relative change of the objective function value is below 0.1%. One can see that the algorithm

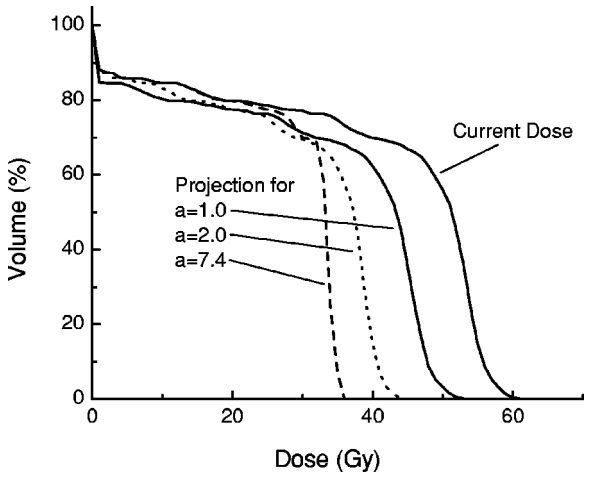

FIG. 4. Example projections for an organ at risk with different organ parameters a.

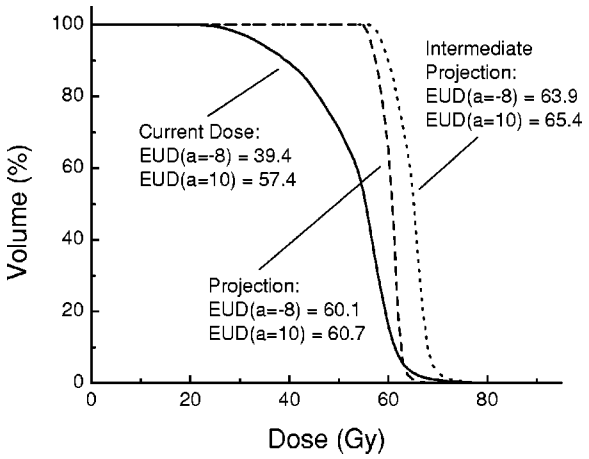

FIG. 5. Example projections for a tumor target structure with maximum and minimum EUD constraints.

interlaces POCS projections and scaled gradient projections. Because all the projections involved are convex, there should be no difference between this approach and a direct one-step projection onto the intensities (however, we have no mathematical proof of that).

III. RESULTS

First, we will look at projections for organs at risk that violate a maximum EUD constraint. As it can be seen from Eq. (16), the projection from the current dose distribution to the one that fulfills the EUD constraint depends on the tissue parameter a. For serial organs, the EUD is mostly determined by the highest voxel doses, so it would have little effect to change the parts of the organ that already receive a low dose. In more parallel organs, the EUD is nearer the mean dose, and the voxels are affected more evenly by the projection. This is shown in Fig. 4. It shows the DVHs of an arbitrary dose distribution in an organ at risk at some point during the optimization, and its projections assuming three different parameters a. The EUD constraint for this organ was set to 33 Gy. Depending on a, the EUD of the current dose distribution is 50.8 Gy ($a=7.4$, which is the parameter for the spinal cord, a mostly serial tissue), 45.4 Gy ($a=2.0$) and 40.9 Gy ($a=1.0$, which represents a parallel tissue architecture). For all three parameters the constraint of 33 Gy was violated, and for each parameter the algorithm has to project to a new dose distribution. For $a=1.0$, the DVH is shifted to the left. For $a=2.0$, the DVH is scaled along the dose axis, and for $a=7.4$, higher doses are effected even more and lower dose parts are not changed at all. The extreme case $a=\infty$ means the equivalence of EUD and physical dose maximum and would lead to the same projection as for maximum dose constraints, cf. Fig. 1. The EUD values of the resulting projections are 32.4 Gy ($a=7.4$), 32.9 Gy ($a=2.0$), and 34.0 Gy ($a=1.0$). One can see that for $a=7.4$ and $a=2.0$ the EUD of the projected dose distribution meets the constraint and is very close to it. Only for $a=1.0$, the EUD of the projection is slightly higher than the constraint. This is because the dose has to be non-negative, and therefore shifting the dose is not completely possible in voxels with a dose $d_i<(\mathrm{EUD}(\mathbf{d})-\mathrm{EUD}^{\mathrm{pres}})$. But this effect is small and becomes even smaller after each iteration when the constraint is reached more closely, and can be neglected.

As stated in the preceding section, for targets the situation is slightly more complicated because there are both minimum and maximum constraints to ensure homogeneity. Two parameters are required, a negative a_- for the minimum EUD constraint and a positive a_+ for the maximum EUD constraint. It is possible that the current dose inside the target violates both constraints, or that the maximum constraint is violated after the projection to the minimum EUD. In these cases two projections directly after one another are necessary. Figure 5 shows an example for a target volume with the constraints $\mathrm{EUD}^{\mathrm{min}}=60\,\mathrm{Gy}\,(a_-=-8)$ and $\mathrm{EUD}^{\mathrm{max}}=61\,\mathrm{Gy}\,(a_+=10)$. First, the minimum EUD constraint is reached by the first projection. Then, the second projection ensures that also the maximum EUD constraint is met.

In the following, we look at optimization results for a clinical head and neck test case using the common physical constraints and the new EUD constraints. A complex shaped target volume, including a boost volume, is located very close to organs at risk: brainstem, spinal cord, and parotid gland. The geometrical situation is illustrated in Fig. 6. The assumption for the planning study was a post-operative irradiation of a carcinoma with unknown primary which became symptomatic because of nodal metastases. The boost/target volumes contain the resection bed and nodal regions. The directions of the seven beams (also indicated in Fig. 6) were selected manually.

Table I shows parameter settings and optimization results. Treatment plan A was calculated with maximum and minimum physical dose constraints for all structures. In treatment plan B the organs at risk were optimized using EUD constraints while keeping the physical constraints for the target and boost, and plan C is the optimization result using EUD constraints for all structures. The slightly more elaborate generation of the prescribed dose array $\mathbf{d}^{\mathrm{pres}}$ for EUD con-

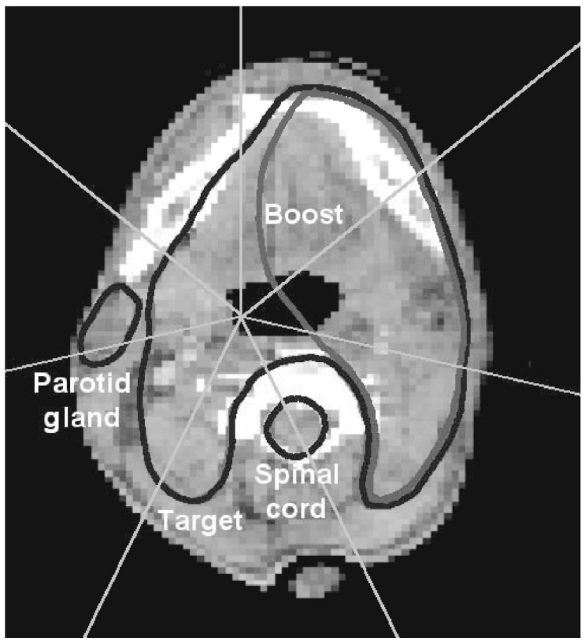

FIG. 6. Exemplary CT slice of the head and neck study case. The outlines of the parotid gland, the spinal cord and the horse-shoe formed target are shown in black, the boost volume in dark gray. Additionally, the directions of the seven beams are indicated. The brain stem is located in more cranial slices, not shown here.

straints [compare Eqs. (3) and (16)] is not noticeable in terms of computation time: The time needed for one single iteration is the same for physical and for EUD constraints; in this specific case this is approximately 7 s on a Pentium IV 1.4 GHz workstation. But the total number of iterations needed increases for EUD constrained optimization, cf. Table I. Figure 7 shows both the DVHs of plan A and plan B. The EUD values of all structures in plan A and the target EUDs in plan

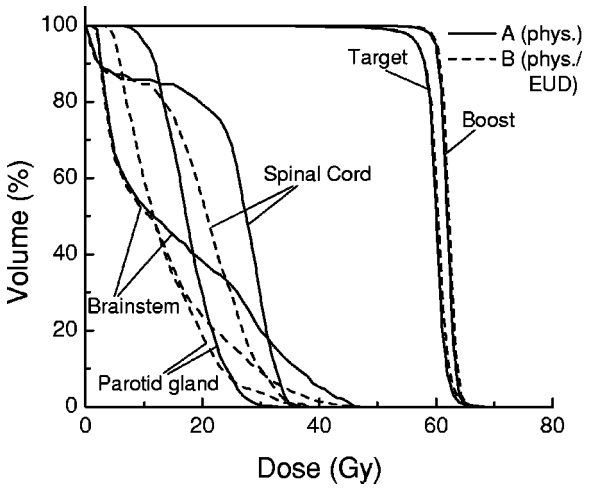

FIG. 7. Optimization results for the head and neck case. Plan A was generated using physical constraints for all structures. For plan B the organs at risk were optimized using maximum EUD constraints.

B are displayed only for informational purposes; they were not used during the optimization. Plan B with EUD constraints shows better sparing of the organs at risk while keeping the dose in the target and boost at the same level as plan A. For the parotid gland (a parallel organ with $a=1$), in plan B the maximum dose values are higher, but the mean dose (and therefore the EUD) is lower. For all structures, the EUD constraints are reached very closely. In Fig. 8 the DVHs of plan C and, again, plan B is shown. The results are similar, but the homogeneity of the target, especially the boost, in plan C is worse than in plan B.

IV. DISCUSSION AND CONCLUSIONS

As can be seen in the results section, the presented algorithm is capable of finding a plan that reaches given EUD

TABLE I. Optimization constraints and results for the head and neck case. All plans were normalized to a target EUD of 58.5 Gy.

	Plan A (physical)	Plan B (physical/EUD)	Plan C (EUD)
Optimization constraints (Gy):			
Target ($a_-=-8$)	D min=60	D min=60	EUD min=60
($a_+=10$)	D max=60	D max=60	EUD max=61
Boost ($a_-=-8$)	D min=62	D min=62	EUD min=62
($a_+=10$)	D max=62	D max=62	EUD max=63
Spinal cord ($a=7.4$)	D max=33	EUD max=25.5	EUD max=25.5
Brainstem ($a=4.6$)	D max=45	EUD max=23	EUD max=23
Parotid gland ($a=1$)	D max=25	EUD max=13	EUD max=13
Result EUD (Gy):			
Target ($a_-=-8$)	58.5	58.5	58.5
($a_+=10$)	60.2	60.5	60.7
Boost ($a_-=-8$)	61.8	62.1	61.6
($a_+=10$)	62.0	62.3	62.7
Spinal cord ($a=7.4$)	28.8	25.8	25.4
Brainstem ($a=4.6$)	27.7	23.1	22.9
Parotid gland ($a=1$)	17.6	13.5	13.0
Iterations	216	309	500

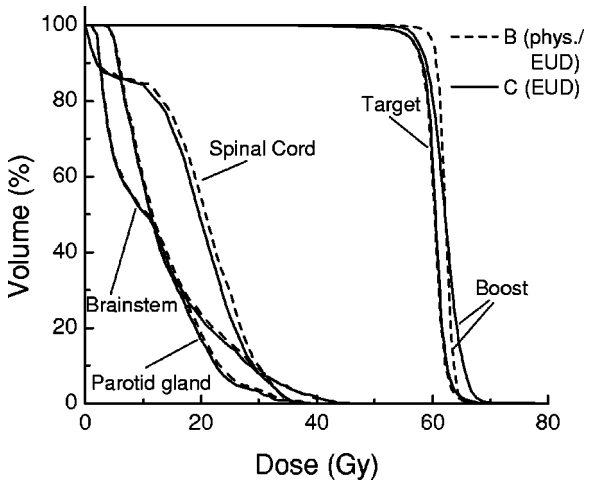

FIG. 8. Again optimization results for the head and neck case. Plan B is the same as in Fig. 7, now compared to plan C where EUD constraints were used for all structures.

constraints closely. It needs more iterations than the physical constrained optimization, but using EUD constraints only for organs at risk, the convergence is still good. Although in our example the EUD constrained optimization shows better sparing of organs at risk than the physical constrained optimization, this cannot be claimed in general. The results depend directly on the concrete constraint settings. Trying more combinations of constraint values and weight factors, better plans might be found. Especially the artificial weight factors have a big impact onto the optimization result which cannot be determined without trial and error. For practical reasons, the process of plan tuning has to stop at some point. The risk of suboptimal plans is inherent to all current inverse planning systems and is independent from the constraint type.

It is also important to note that the EUD of an organ at risk is not optimized beyond the constraint (in contrast to the method described in Ref. 7). Without further modifications to the algorithm, the planner has to define a sufficiently low constraint to minimize the EUD as much as possible.

The same optimization result as in plan B could have been also reached with a set of DVH constraints. Additional case comparisons would be necessary to assess more thoroughly the differences between EUD-based and DVH-based optimization in terms of efficiency and overall plan acceptability. The fact that EUD constraints can lead to a better overall result in the organs at risk than simple maximum dose constraints becomes plausible by looking at Figs. 1 and 4: Whereas no voxel below the maximum dose constraint is optimized (see Fig. 1), the EUD constraint affects, depending on the organ parameter, much more or even all voxels of the organ (see Fig. 4). It is recognized, of course, that it is always necessary to accept either higher maximum dose in the organ at risk or lower dose in the planning target volume if these two volumes are in contact with each other or approach each other so closely that it is impossible to configure a beam orientation providing adequate dose fall-off between the structures, no planning system can overcome this intrinsic difficulty.

The question is where the use of EUD constraints is most suitable and how they compare to the physical constraints. From Eq. (6) one can see that when a is positive infinity (completely serial organ), the EUD equals the maximum dose in the structure. In this case, the POCS method projects exactly onto the maximum dose constraint, so the use of ''maximum physical dose constraint'' and ''maximum EUD constraint'' is equivalent. In analogy, a set to negative infinity (where the EUD equals the minimum dose) implies the equivalence of a minimum EUD constraint and a pure physical dose minimum constraint. In that sense the pure physical maximum/minimum dose constraints are a subset of EUD constraints, namely for structures with a set to $\pm\infty$.

The differences become bigger and bigger when the organ structure becomes more and more parallel (cf. parotid gland in Fig. 7), indicating that a physical maximum dose constraint is no longer sufficient. Especially for these organs, either DVH constraints or EUD constraints should be used. The EUD constraint is easier to define and does not imply a predefined shape of the DVH. The optimization will find the dose distribution that is best adapted to the specific case. As found in the results section, even for organs considered as mostly serial (like the spinal cord) EUD constraints can improve the optimization result.

EUD constraints for target structures using organ parameters as in plan C resulted in more iterations, probably because for targets there can be two POCS projections in one iteration, which is not the case in standard POCS algorithms (see Material and Methods). The dose homogeneity is also lower. So for targets the use of higher a_+ (for the maximum EUD constraint) and lower a_- (for the minimum EUD constraint) organ parameters up to positive/negative infinity seems more suitable.

One main advantage of the algorithm presented in this work is that it is very close to the existing physical optimization. It is easy to integrate into any inverse planning system that uses a gradient optimization technique and voxel based dose constraints. Virtually nothing of the existing system has to be changed; the EUD constraint is just an additional feature and is realized by a simple plug-in, cf. Fig. 3.

The other main advantage is that for every organ or structure the planner can decide separately what kind of constraint should be used. It is not necessary to change the whole planning paradigm. Inverse planning is a process that requires a lot of experience from the planner, and the introduction of EUD constraints as presented does not render this experience obsolete. Instead, it is possible to make use of the EUD concept in a conservative way by using an EUD constraint only for selected organs, and use physical dose constraints and the knowledge about the correct settings for constraints and penalty factors for all other organs. This ensures a smooth transition from a pure physical dose oriented to a clinical more meaningful optimization. Because the EUD for organs at risk is an empirical model, the clinical relevance of EUD directly corresponds to the quality of the clinical data (dose distributions and their clinical effects) available. The more and more three-dimensional treatment planning and documentation becomes clinical routine, one can expect that the relevance of

EUD and the validity of the model parameters will increase. The usefulness of a smooth transition is also supported by the fact that planning based on TCP/NTCP models was introduced several years ago[20,21] but is still not widely used in clinical practice. The EUD is an intermediate concept between physical doses and TCP/NTCP models. It is still in the dose domain, and its implementation shown in this paper does not cope with, but on the other hand is also not affected by the uncertainties of dose-effect relationships. Inverse planning based on the probabilities of tumor control and normal tissue complication remains the ultimate goal, and the equivalent uniform dose is a step in this direction.

ACKNOWLEDGMENTS

We would like to thank Professor Yair Censor for his thoughtful comments on the paper. We also thank Dr. Dr. J. Debus and his staff at the Clinical Cooperation Unit Radiation Oncology, German Cancer Research Center Heidelberg, for providing the presented clinical data. This work was supported by Grant No. CA 50628 from the National Cancer Institute, DHHS.

[1] A. Pugachev, J. G. Li, A. L. Boyer, S. L. Hancock, Q. T. Le, S. S. Donaldson, and L. Xing, ''Role of beam orientation optimization in intensity-modulated radiation therapy,'' Int. J. Radiat. Oncol., Biol., Phys. **50**, 551–560 (2001).

[2] T. Bortfeld, ''Optimized planning using physical objectives and constraints,'' Semin Radiat. Oncol. **9**, 20–34 (1999).

[3] T. Bortfeld, J. Stein, and K. Preiser, ''Clinically relevant intensity modulation optimization using physical criteria,'' in *The Use of Computers in Radiation Therapy* (ICCR 1997), edited by G. Starkschall and D. D. Leavitt (Medical Physics Publishing, Madison, WI, 1997), pp. 27–30.

[4] A. Niemierko, ''A generalized concept of equivalent uniform dose,'' Med. Phys. **26**, 1100 (1999).

[5] A. Niemierko, ''Reporting and analyzing dose distributions: A concept of equivalent uniform dose,'' Med. Phys. **24**, 103–110 (1997).

[6] B. Emami *et al.*, ''Tolerance of normal tissue to therapeutic irradiation,'' Int. J. Radiat. Oncol., Biol., Phys. **21**, 109–122 (1991).

[7] Q. Wu, R. Mohan, A. Niemierko, and R. Schmidt-Ullrich, ''Optimization of intensity-modulated radiotherapy plans based on the equivalent uniform dose,'' Int. J. Radiat. Oncol., Biol., Phys. **52**, 224–235 (2002).

[8] S. Nill, ''Development and application of a multi-modality inverse treatment planning system,'' Ph.D. thesis, Ruprecht–Karls–Universitaet Heidelberg, Germany, 2001.

[9] K. Preiser, T. Bortfeld, K. Hartwig, W. Schlegel, and J. Stein, ''A new program for inverse radiotherapy planning,'' in *The Use of Computers in Radiation Therapy* (ICCR 1997), edited by G. Starkschall and D. D. Leavitt (Medical Physics Publishing, Madison, WI, 1997), pp. 425–428.

[10] C. Scholz, S. Nill, U. Oelfke, and T. Bortfeld, ''Application of an advanced photon dose algorithm for inverse IMRT planning,'' Med. Phys. **29**, 1335 (2002).

[11] P. S. Cho and M. H. Phillips, ''Reduction of computational dimensionality in inverse radiotherapy planning using sparse matrix operations,'' Phys. Med. Biol. **46**, N117–N125 (2001).

[12] C. Thieke, S. Nill, U. Oelfke, and T. Bortfeld, ''Acceleration of intensity-modulated dose calculation by importance sampling of the calculation matrices,'' Med. Phys. **29**, 676–681 (2002).

[13] C. Thieke, T. Bortfeld, and K. H. Kuefer, ''Characterization of dose distributions through the max and mean dose concept,'' Acta Oncol. **41**, 158–161 (2002).

[14] B. Choi and J. O. Deasy, ''The generalized equivalent uniform dose function as a basis for intensity-modulated treatment planning,'' Phys. Med. Biol. **47**, 3579–3589 (2002).

[15] L. M. Bregman, ''Finding the common point of convex sets by the method of successive projections,'' Dokl. Akad. Nauk UzSSR **162**, 487–490 (1965).

[16] L. G. Gubin, B. T. Polyak, and E. V. Raik, ''The method of projections for finding the common point of convex sets,'' USSR Comput. Math. Math. Phys. **7**, 1–24 (1967).

[17] D. C. Youla and H. Webb, ''Image restoration by the method of convex set projections: Part I-Theory,'' IEEE Trans. Med. Imaging **MI-1**, 81–94 (1982).

[18] S. Lee, P. S. Cho, R. J. Marks II, and S. Oh, ''Conformal radiotherapy computation by the method of alternating projections onto convex sets,'' Phys. Med. Biol. **42**, 1065–1086 (1997).

[19] P. S. Cho, S. Lee, R. J. Marks II, S. Oh, S. G. Sutlief, and M. H. Phillips, ''Optimization of intensity modulated beams with volume constraints using two methods: Cost function minimization and projections onto convex sets,'' Med. Phys. **25**, 435–443 (1998).

[20] S. Sodertrom and A. Brahme, ''Optimization of the dose delivery in a few field techniques using radiobiological objective functions,'' Med. Phys. **20**, 1201–1210 (1993).

[21] A. Niemierko, M. Urie, and M. Goitein, ''Optimization of 3D radiation therapy with both physical and biological end points and constraints,'' Int. J. Radiat. Oncol., Biol., Phys. **23**, 99–108 (1992).